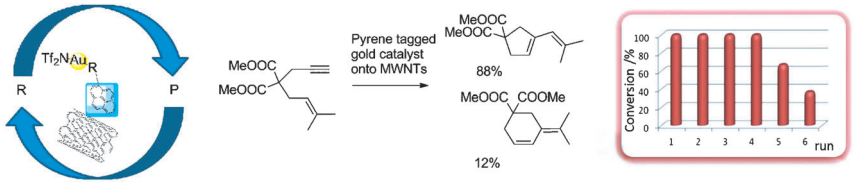

Recycling the boomerang: A pyrene-tagged gold complex has been synthesised and immobilised onto multi-walled carbon nanotubes (MWNTs) through π–π stacking interactions. The catalyst displays good catalytic activity in a number of enyne cyclisation reactions (see figure). The recyclability by heterogeneous catalysis and the boomerang effect was evaluated. Under the optimised conditions, recycling is possible when the boomerang system is used and provides the first example of a supported gold catalyst on carbon nanotubes.

Supported Catalysts

C. Vriamont, M. Devillers, O. Riant, S. Hermans** ..... ▮▮▮▮–▮▮▮▮

Catalysis with Gold Complexes Immobilised on Carbon Nanotubes by π–π Stacking Interactions: Heterogeneous Catalysis versus the Boomerang Effect

CHEMISTRY
A EUROPEAN JOURNAL

ChemPubSoc
Europe

DOI: 10.1002/chem.201300998

Catalysis with Gold Complexes Immobilised on Carbon Nanotubes by π–π Stacking Interactions: Heterogeneous Catalysis versus the Boomerang Effect

Charles Vriamont, Michel Devillers, Olivier Riant,* and Sophie Hermans*[a]

Abstract: A new pyrene-tagged gold(I) complex has been synthesised and tested as a homogeneous catalyst. First, a simple 1,6-enyne was chosen as a model substrate for cyclisation by using different solvents to optimise the reaction conditions. The non-covalent immobilisation of our pyrene-tagged gold complex onto multi-walled carbon nanotubes through π–π stacking interactions was then explored to obtain a supported homogeneous catalyst. The heterogenised catalyst and its homogeneous counterpart exhibited similar activity in a range of enyne cyclisation reactions. Bearing in mind that π–π interactions are affected by temperature and solvent polarity, the reuse and robustness of the supported homogeneous catalyst was tested to explore the scope and limitations of the recyclability of this catalyst. Under the optimised conditions, recyclability was observed by using the concept of the boomerang effect.

Keywords: gold · nanotubes · pi interactions · recycling · supported catalysts

Introduction

Supported homogeneous catalysis, that is, the immobilisation of a homogeneous catalyst onto a solid support, allies advantages of both homogeneous and heterogeneous catalysis. A highly active and well-characterised catalyst combined with the possibility of separating it from products, allowing their possible use in continuous flow processes, is very attractive. This "heterogenisation" can be conducted by different routes 1) the formation of covalent bonds between the support and the complex, 2) adsorption or ion pairing with the support and 3) encapsulation. Many of these strategies have already been implemented for the immobilisation of various metal complexes on to different materials such as MCM, zeolites and polymers.[1–6] Surprisingly, the expected emergence of these molecular catalysts on carbon nanotubes (CNTs) has not yet appeared despite the rich chemistry associated with the functionalisation of these tubes.[7]

CNTs possess remarkable properties such as high chemical and thermal stability and conductivity, resistance to acid and basic media, and the possibility of being functionalised by a large—and not yet fully tested—variety of chemical reagents. Their functionalisation can be divided into three families: defect-site functionalisation, covalent sidewall functionalisation and non-covalent functionalisation. The most referenced is the covalent approach, which comprises reductive alkylation, cycloadditions, carbene or nitrene addition, reactions involving radicals or the well-known functionalisation of carboxylic acid groups obtained by the oxidative treatment of CNTs.[8–11] These covalent functionalisation strategies modify the carbon hybridisation from sp^2 to sp^3 and therefore lead to a partial or total loss of the intrinsic properties of the pristine carbon nanotubes, which is in contrast to non-covalent functionalisation. The non-covalent modification of carbon nanotubes is of growing interest and different types of molecular structures can be immobilised onto CNTs, such as aromatic small molecules (pyrene, porphyrin and their derivatives), biomacromolecules (proteins, enzymes, DNA, (poly)saccharides, etc) and polymers. This strategy has been applied to various areas of interest, such as nanoelectronics, nanomaterials science, drug delivery and catalysis.[12–15] We have chosen carbon nanotubes as a support for homogeneous catalysts for their potential to interact strongly with polyaromatics through non-covalent π–π interactions. The selected method has some non-negligible advantages compared with covalent functionalisation. It is simpler because the initial functionalisation of CNTs before anchoring of the catalyst is not required. Moreover, the use of a non-polar solvent provides a simple and convenient way of recovering both the intact catalyst and the nanotubes unaltered. The preliminary choice of a pyrene-tagged group is of critical importance for the immobilisation of catalysts. Some studies relating to π–π stacking have been carried out and indicated that stacked structures become increasingly favourable with increasing arene size. Systems such as pyrene or coronene show π–π stacking with the hydrogen atoms located roughly over ring centres.[16,17] Pyrene seems to be the smallest molecular unit able to interact non-covalently with carbon nanotubes. Compared with coronene or larger arenes able to perform the same interactions, we se-

[a] C. Vriamont, Prof. M. Devillers, Prof. O. Riant, Prof. S. Hermans
Institute of Condensed Matter and Nanosciences,
Molecules, Solids and Reactivity (IMCN/MOST)
Université catholique de Louvain
Place Louis Pasteur 1, 1348 Louvain-la-Neuve (Belgium)
Fax: (+32) 10-472330
E-mail: olivier.riant@uclouvain.be
sophie.hermans@uclouvain.be

Supporting information for this article is available on the WWW under http://dx.doi.org/10.1002/chem.201300998.

lected pyrene as the smallest unit in the hope of optimising the catalyst immobilisation on CNTs per unit surface area.

Homogeneous gold catalysis has been blooming during the past ten years since this metal has had a resurgence.[18–23] Gold has been identified as a captivating metal able to play in a wide range of chemical transformations,[24–30] such as enyne cycloisomerisation,[31–41] hydroamination,[40,42,43] hydroalkoxylation,[44] alkyne hydration,[45] benzannulation,[46] furan/yne cyclisation[47] or hydrophosphoryloxylation.[48] However, despite their excellent reactivity allowing low catalyst loading, gold complexes are quite expensive and therefore their potential reuse is of critical importance.

To the best of our knowledge only a few publications have described the covalent anchoring of molecular catalysts on to CNTs[49–58] and even fewer with a non-covalently immobilised molecular catalyst through π–π interactions.[59–62] Despite some elegant applications in catalysis, little reliable quantitative data is available regarding the immobilisation capacities of CNTs for homogeneous catalysts. Liu et al. reported the immobilisation of pyrene-tagged ruthenium carbene complexes for ring-closing metathesis, but their quantification was based only on UV titration of the non-immobilised complexes.[59] In a closely related study, Reiser and coworkers reported an elegant method for immobilising palladium complexes on to carbon-coated magnetic cobalt nanoparticles.[63]

We report herein the synthesis of a pyrene-tagged gold complex as well as a study of its non-covalent immobilisation on to carbon nanotubes through π–π stacking. The immobilised complex was fully characterised and studied in some selected benchmark reactions to assess and quantify its potential recyclability.

Results and Discussion

Synthesis of the pyrene-tagged gold complex: The desired bifunctional pyrene ligand was obtained according to the synthetic route outlined in Scheme 1. A halogen/lithium exchange reaction between 4-bromobenzonitrile (**1**) and *n*BuLi followed by trapping with chlorodiphenylphosphine gave the corresponding phosphine **2**. $LiAlH_4$ reduction of the nitrile group yielded the corresponding amine **3**,[64] which was finally coupled with 1-pyrenebutyric acid to give the bifunctional ligand **4** in an overall yield of 55% for the three steps. This air-stable ligand **4** could thus be easily prepared on a multi-gram scale and was fully characterised (mass spectrometry, ^1H, ^{13}C and ^{31}P NMR, see the Supporting Information).

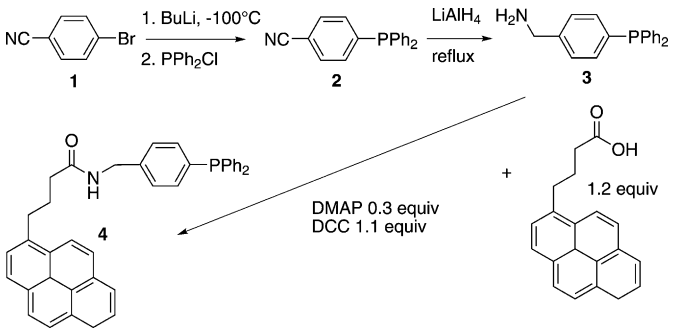

Scheme 1. Synthesis of the bifunctional ligand **4**.

Ligand exchange between ligand **4** and the commercially available chloro(dimethylsulfide)gold(I) complex allowed us to obtain **5** (Scheme 2). The desired pyrene-tagged gold catalyst **6** was finally obtained by treating complex **5** with 1 equivalent of $AgNTf_2$ in an overall yield of 40% starting from **1**. This complex was extensively characterised by thermal gravimetric analysis (TGA), HRMS and ^{19}F, ^{31}P, ^{13}C and ^1H NMR spectroscopy (see the Supporting Information). The bis(trifluoromethanesulfonyl)imidate moiety was chosen as the weakly coordinating counter anion because it is a valuable candidate for the synthesis of stable gold(I) catalysts. Such complexes are known to be stable, non-hygroscopic and highly active as catalysts for a wide range of reactions such as enyne cycloisomerisations.[37]

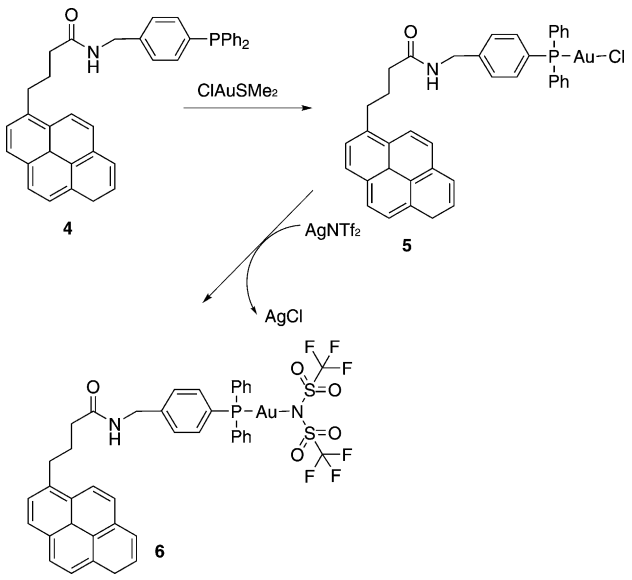

Scheme 2. Synthesis of the pyrene-tagged gold complex **6**.

Incorporation and immobilisation of the gold complex 6 onto multi-walled carbon nanotubes (MWNTs): The pyrene group is important, as mentioned above, for non-covalently immobilising a homogeneous catalyst onto a CNT. Due to the lipophilicity of both pyrene and MWNTs, the use of a polar solvent would seem to be required to maintain the π–π interactions during the immobilisation step.[16] Complex **6** is soluble in most common polar solvents. Acetone was chosen to study the incorporation of **6** onto carbon nanotubes with time (Scheme 3). The MWNTs were dispersed in the solvent in an ultrasound bath before the addition of **6** and magnetic stirring for various periods of time (from a few minutes to a few hours). Finally, the mixtures were sub-

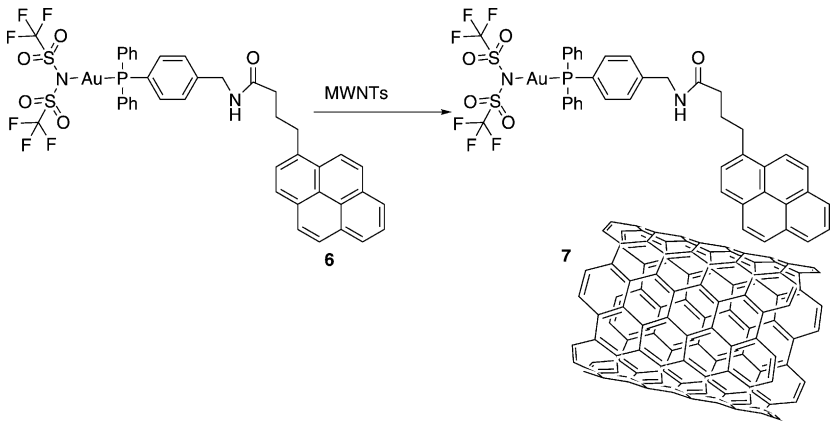

Scheme 3. Incorporation of the pyrene-tagged gold complex **6** onto MWNTs.

jected to centrifugation to separate the functionalised MWNTs (*f*-MWNTs) **7** from the liquid phase. The solutions were analysed by inductively coupled plasma (ICP) (Table 1), which showed that the majority of introduced **6** was indeed incorporated on to the MWNTs irrespective of the time. The highest degree of incorporation of **6** was observed after 60 min. The solids were analysed by X-ray photoelectron spectroscopy (XPS). Based on the surface gold atomic percentage, this analysis showed that complex **6** is indeed incorporated on to the MWNTs to give **7** irrespective of the incorporation time (see Table S1 in the Supporting Information). The other elements in the gold complex (F, N, P, S) were also analysed. The experimental ratios between these elements and gold are close to the theoretical numbers (Table 1), which indicates that the complex remains intact after incorporation. The best values were found after 60 and 300 min. On the basis of these results, an incorporation time of 60 min was chosen. Figure 1 shows both the XPS spectra of pristine MWNTs and functionalised MWNTs **7** after 60 min. This latter spectrum shows the presence of the desired elements (F, N, S, P, Au) and evidence that the oxidation state of gold remains Au^{I} after incorporation.

Table 1. ICP and XPS data after the incorporation of **6** onto MWNTs after different periods of time.

Incorporation time [min][a]	Au remaining in solution [%][b]	Au/C[c]	F/Au	N/Au	P/Au	S/Au
20	26.4	3.4	7.04	3.42	0.88	2.22
60	12.5	4.6	7.06	2.39	0.93	1.81
160	16.5	3.3	7.51	2.10	0.80	2.43
210	26.4	3.4	9.67	3.39	1.00	2.85
300	22.4	3.5	6.82	1.84	0.84	2.09
1440	26.4	4.5	8.84	2.17	0.75	2.33
calculated ratio	–	–	6	2	1	2

[a] Experimental conditions. [b] Determined by ICP analysis of the filtrates. [c] Value × 1000.

The incorporation procedure was performed in different solvents such as acetonitrile, acetone and dichloromethane to identify the best medium for incorporation and to determine whether the use of a polar solvent was necessary (Table 2). The manipulations were carried out a number of times with different quantities of reagent (from 15 to 100 mg) to verify the reproducibility. In all cases, the ratios between the different elements (F, N, P, and S) and gold determined by XPS were similar and close to the calculated values. The XPS ratio of gold/carbon fluctuates between 0.0027 and 0.0037, which indicates that the methodology is reproducible. However, this ratio seems lower when acetonitrile was used. Complex **6** was analysed by ^{31}P NMR spectroscopy over time to verify its stability in these three solvents (see the Supporting Information). The ^{31}P NMR spectra show the appearance of a second minor peak in acetone and acetonitrile that is not present in dichloromethane; this second peak does not correspond to either an oxidised species or the free ligand and remains unassigned, however, it must be due to a new complex formed by rearrangement. For these reasons, dichloromethane was chosen as the best compromise between quantity, quality of incorporation and stability of the complex. The sample prepared in dichloromethane was characterised by nitrogen physisorption and the data compared with the starting MWNTs (see Table S3 and Figure S13 in the Supporting Information). As expected, the specific surface area (S_{BET} and S_{BJH}) and pore volume were found to decrease after the immobilisation of **6**. Indeed, the layer of immobilised compounds on the CNTs fills the voids that existed previously between entangled nanotubes. The average pore size, however, was found to increase, probably due to blocking of the smallest micropores (defects and opening of the internal cavity) by adsorbed gold complex molecules.

ICP analysis was performed on some samples to determine the bulk amount of gold on the CNT supports (Table 3 and Table S2 in the Supporting Information for all values). The results showed between 0.12 and 0.22 mmol of **7** per g of the MWNTs, which clearly demonstrates that a non-negligible amount of the catalyst **6** was incorporated onto the MWNTs by a non-covalent pathway.

As already mentioned in the introduction, only four publications have reported the immobilisation of a molecular catalyst on to MWNTs through π–π interactions.[59–62] Two of them focused on the immobilisation of pyrene-functionalised electroactive transition-metal complexes on to electrode-supported CNTs for electrocatalysed reactions. In the two remaining references, UV titration with the pyrene fingerprint was used to determine the quantity of immobilised catalyst. The metal loading of these complexes on carbon nanotubes was compared with the values we obtained for our gold complex determined by ICP; the reported values

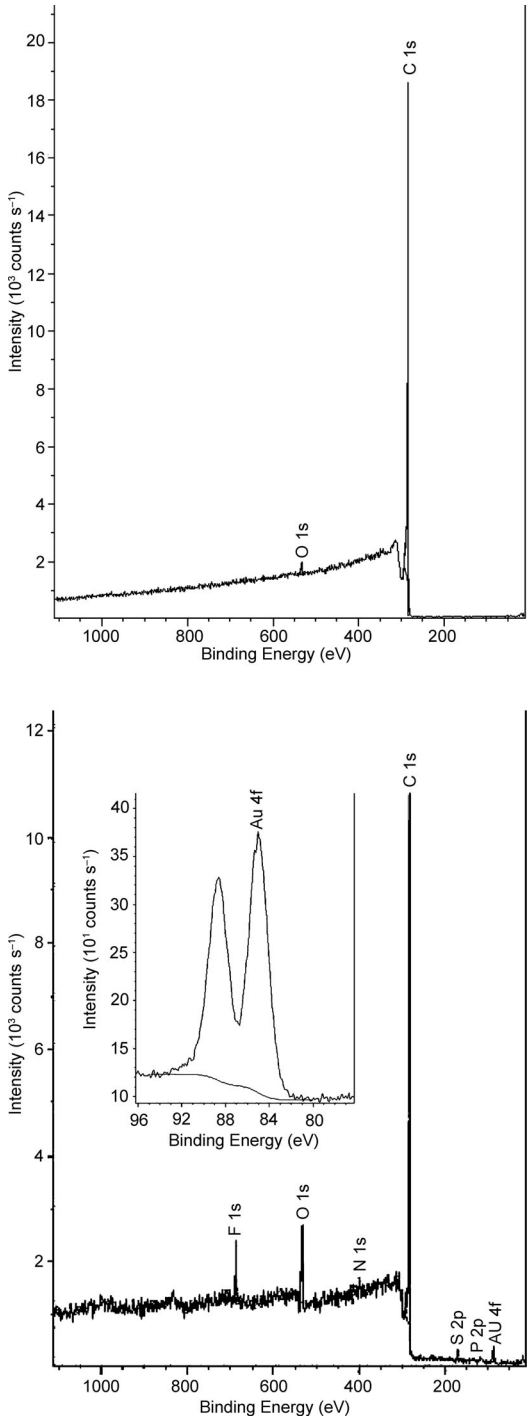

Figure 1. XPS spectra of pristine MWNTs (top) and f-MWNTs **7** (bottom). Inset: Gold narrow scan.

Table 2. Incorporation of **6** onto MWNTs in various solvents.

Entry	Solvent	Au/C[a]	F/Au	N/Au	P/Au	S/Au
1	acetone[b]	3.65	6.92	2.04	0.96	2.11
2	CH_2Cl_2	3.35	7.70	2.39	0.95	2.54
3	CH_3CN	2.72	6.17	1.83	1.12	2.23

[a] Value $\times 1000$. [b] Average of eight experiments (all values are reported in the Supporting Information).

Table 3. ICP values for the loading of **7** and some literature supported homogeneous catalysts immobilised covalently or non-covalently onto CNTs.

Entry	Metal	Immobilisation methodology	Immobilisation loading[a]	Ref.
1	Au	π–π interactions	0.12–0.22 (ICP)	this work
2	Rh	π–π interactions	0.17 (UV)	[61]
3	Ru	π–π interactions	0.16 (UV)	[59]
4	V	covalent	0.08 (ICP)	[53]
5	Mo	covalent	0.25–0.35 (ICP)	[54]
6	W	covalent	0.03 (ICP)	[56]
7	Mn	covalent	0.06 (ICP)	[57]
8	Mn	covalent	0.14 (ICP)	[58]

[a] Units: mmol catalyst per g of CNTs. Techniques used to determine the metal loading are given in parentheses.

lie in the range of our results (Table 3). Note that, to the best of our knowledge, the only other paper describing π–π stacking between CNTs and a pyrene-tagged complex of terbium (single molecular magnets) reported an ICP value of 0.28 mmol of terbium complex per g of CNT.[65] In order to compare **7** with a wider range of catalysts, a particular attention was focused on molecular catalysts covalently bonded to carbon nanotubes. The most outstanding examples determined by ICP are listed in Table 3; the loading of **7** between 0.12 and 0.22 mmol g^{-1} falls in the range of covalently and non-covalently CNT supported homogeneous catalysts reported in the literature.

Catalytic tests: Optimisation of homogeneous catalysis: Complex **6** was first tested as a homogeneous catalyst to prove its activity in well-mastered representative reactions in the field of gold chemistry. The simple enyne **8** was initially chosen as a model substrate for cyclisation (Table 4), and different solvents were used to optimise the reaction conditions. Complex **6** was active in the cyclisation of enyne **8** and gave complete conversion with dichloromethane or acetone as solvent. Interestingly, a change of solvent induced a change in the outcome of the reaction. The use of dichloromethane predominantly gave the 5-*exo*-dig product **9** and a minor amount of the 6-*endo*-dig product **10** in a ratio of 88:12. When acetone was used, product **9** was again predominant with a minor amount of **10**, but the side-product **11** was also formed, probably due to the inherent pres-

Table 4. Effect of solvents on the cycloisomerisation of enyne **8**.

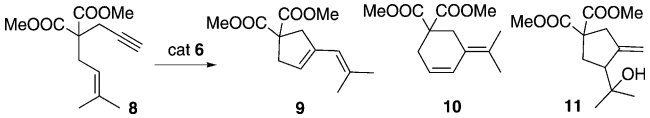

Entry	Solvent	Catalyst **6** [mol%]	t [h]	T [°C]	Conversion [%] (products, ratio)
1	CH_2Cl_2	2	0.5	RT	100 (**9**+**10**, 88:12)
2	acetone	2	1	35	100 (**9**+**10**+**11**)[a]
3	CH_3CN	2	24	35	0
4	DMF	2	24	35	0
5	MeOH	2	24	RT	0

[a] No ratio is indicated because other side-products were also observed.

ence of water in acetone (see the Supporting Information). Furthermore, when acetone was used, a longer reaction time and higher temperature were needed to reach quantitative conversion. Finally, when other polar solvents were used (CH_3CN, DMF, MeOH), no conversion was observed.

On the basis of these results, dichloromethane was selected as the solvent for a small collection of benchmark substrates, that is, enynes **8** and **12–15** and the propargylic carbonates **16** and **17** (Scheme 4).[34,66–68] The cyclisations of substrates **8** and **12–16** proceeded readily at room temperature in CH_2Cl_2 with a 2 mol% catalytic loading of **6** and

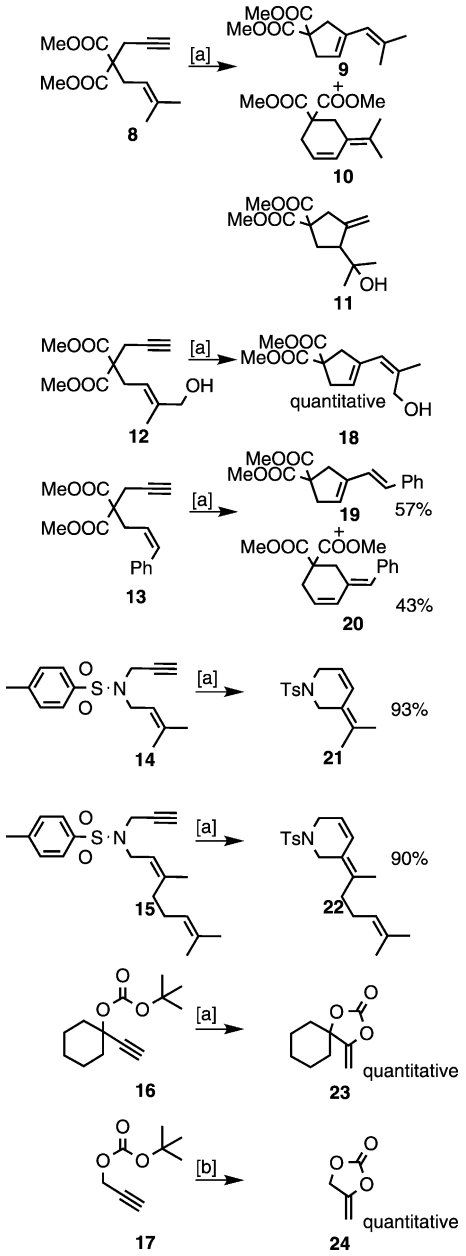

Scheme 4. Cyclisation of enynes and propargylic carbonates with gold complex **6**. Reagents and conditions: CH_2Cl_2 (acetone for molecule **8**), 2 mol% **6**, room temperature (35 °C when acetone was used), [a] 30 min; [b] 7 h.

were complete in 30 min. A longer time, that is, 7 h, was required for the cyclisation of **17**. The rearrangement was stereospecific for enyne **12** with a Z configuration of the alkene, giving the Z-diene **18** quantitatively.[34] The enyne **13** was quantitatively cyclised to give a mixture of two products by an exohedral (**19**) and endohedral (**20**) skeletal rearrangement in a ratio of 57:43, respectively. The *N*-toluene-4-sulfonyl derivatives **14** and **15** both underwent exohedral rearrangement and were converted into **21** and **22**, respectively. In both cases, the conversion was equal to or higher than 90%. A longer reaction time did not increase the conversion rate. Finally, the propargylic carbonates **16** and **17** were quantitatively transformed into the known methylene carbonates **23** and **24**.[71]

Supported homogeneous catalysis: Once the reactivity of **6** as catalyst in the model reactions had been demonstrated, catalyst **7** was tested to compare its activity and selectivity with its homogeneous counterpart **6**. The results obtained are presented in Table 5. The supported catalyst displayed

Table 5. Comparison of **6** and **7** as catalysts in the homogeneous and heterogeneous catalytic reactions.

Entry	Substrate	Catalyst	Solvent	Products (yield[a] [%], ratio[b])
1	**8**	**6**	acetone	**9**+**10**+**11**
2	**8**	**7**	acetone	**9**+**10**+**11**
3	**8**	**6**	CH_2Cl_2	**9**+**10** (100, 88:12)
4	**8**	**7**	CH_2Cl_2	**9**+**10** (100, 88:12)
5	**12**	**6**	CH_2Cl_2	**18** (100)
6	**12**	**7**	CH_2Cl_2	**18** (100)
7	**13**	**6**	CH_2Cl_2	**19**+**20** (100, 57:43)
8	**13**	**7**	CH_2Cl_2	**19**+**20** (100, 57:43)
9	**14**	**6**	CH_2Cl_2	**21** (93)
10	**14**	**7**	CH_2Cl_2	**21** (93)
11	**15**	**6**	CH_2Cl_2	**22** (90)
12	**15**	**7**	CH_2Cl_2	**22** (90)
13	**16**	**6**	CH_2Cl_2	**23** (100)
14	**16**	**7**	CH_2Cl_2	**23** (100)
15	**17**	**6**	CH_2Cl_2	**24** (100)
16	**17**	**7**	CH_2Cl_2	**24** (100)

[a] Isolated yield. [b] Measured by ^{1}H NMR analysis of the crude reaction mixture. Cyclisation of molecules with gold complex **6** and supported catalyst **7**. Reagents and conditions: CH_2Cl_2 (acetone for molecule **8**), 2 mol% **6** or **7**, room temperature (35 °C when acetone was used), 30 min (**8**, **12–16**) or 7 h (**17**).

good catalytic activity and gave the same conversion as its homogeneous counterpart irrespective of the solvent. Furthermore, the same selectivity was observed towards the skeletal rearrangement in the cyclisation of enynes **8** and **13**. These results suggest that the support does not play a role during the catalysis. The absence of steric or electronic effects is probably due to the long distance between the active site for catalysis, which is the Au^I atom, and the pyrene moiety in interaction with nanotubes.

Recyclability of the supported homogeneous gold catalyst: In view of the excellent results obtained with the heterogenised catalyst **7**, the ultimate goal was to explore its recycla-

bility in the two media used during this work, acetone and dichloromethane. In both cases the supported homogeneous catalyst **7** (2 mol% based on ICP values) was first subjected to ultrasound before addition of substrate **8** in acetone or substrates **8** and **14** in dichloromethane. After 30 min, the cyclisation products were separated from the *f*-MWNTs **7** by centrifugation. This was carried out at room temperature in acetone, but in dichloromethane the solution was first cooled to −40 °C before centrifugation. The recovered catalysts were then ready for a new catalytic run, and the solution containing the products was analysed by ^{1}H NMR spectroscopy. The recyclability in acetone was tested a couple of times and gave unambiguous results: the second run did not give any cyclisation products with the model substrate **8**, which indicates that deactivation had occurred. The recyclability of the catalyst in the reactions of enynes **8** and **14** in dichloromethane gave good results (Schemes 5 and 6).

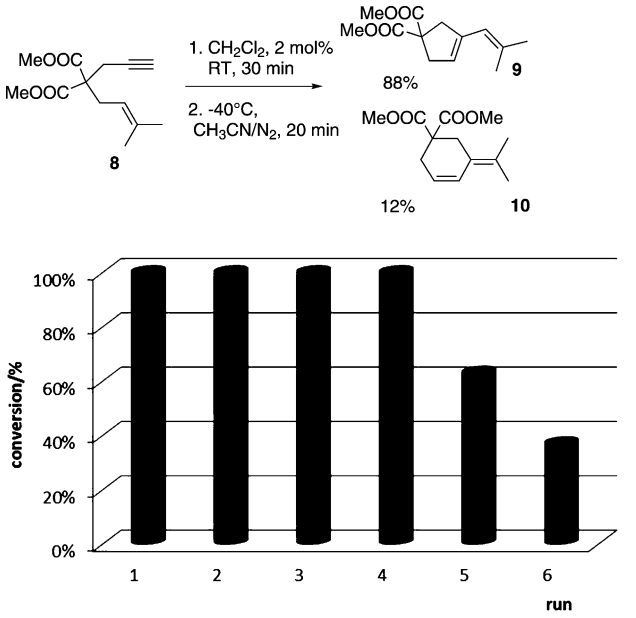

Scheme 5. Recycling of catalyst **7** (2 mol%) in the cyclisation of enyne **8**.

Indeed, four successive catalytic runs were accomplished with quantitative cyclisation of enyne **8** into the corresponding *exo* and *endo* products **9** and **10** (ratio 88:12) without any loss of catalytic activity. However, loss of activity was observed during runs 5 and 6, with conversions of 67 and 37%, respectively (Scheme 5). The ratio between the two cyclised products remained unchanged during each run. The cyclisation of enyne **14** into the corresponding product **21** was also tested. A slow decrease in the conversion was observed during the first four runs before an abrupt fall during the fifth run. Conversions of 93, 83, 63, 56 and finally 6% for the final run were observed (Scheme 6).

Heterogeneous catalysis versus Boomerang effect: Liu[59] and Reiser[63] and their co-workers showed that π–π stacking interactions between pyrene and nanotubes are affected by

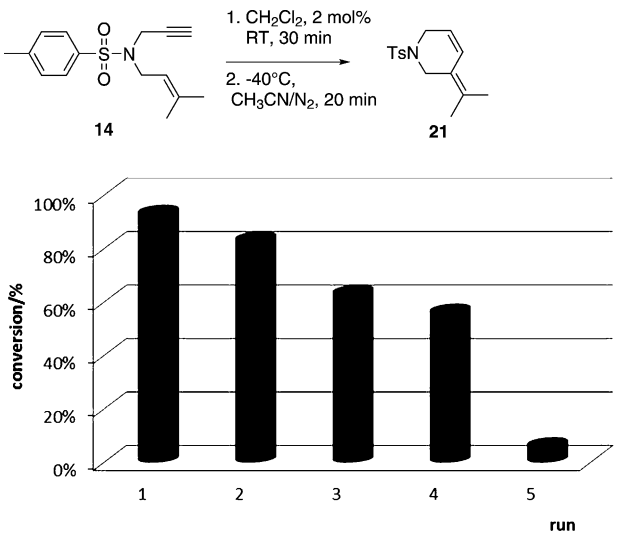

Scheme 6. Recycling of catalyst **7** (2 mol%) in the cyclisation of enyne **14**.

the polarity of the solvent and by the temperature. These two approaches are conceivable and are presented in Scheme 7. The first pathway (right) shows the pyrene-tagged gold complex strongly immobilised onto the CNTs during catalysis and easily separable from the products once the reaction is finished, that is, acting as a heterogeneous catalyst due to the polar nature of the solvent. The second pathway (left), in a non-polar solvent, involves a boomerang effect: the gold complex acts as a homogeneous catalyst before being re-immobilised onto the CNTs following a lowering of the temperature (from room temperature to −40 °C). These two pathways were tested with varying degrees of success based on the results of the recyclability study described above. To test the concept of heterogeneous catalysis, acetone was used as the polar medium. Indeed, the

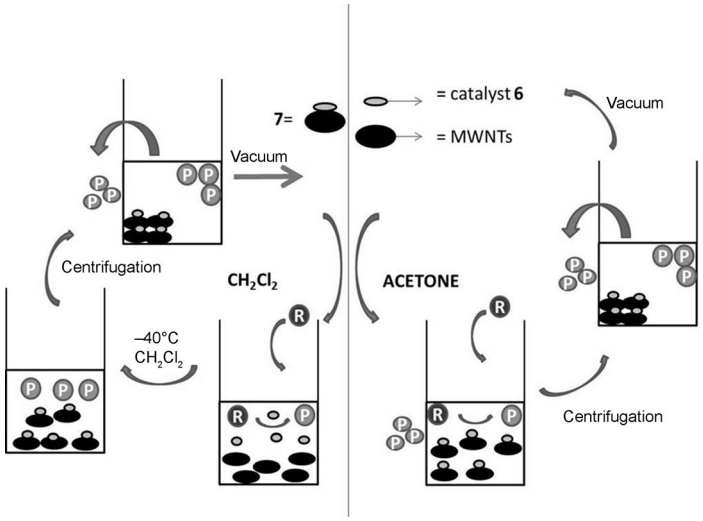

Scheme 7. Mechanisms for the boomerang effect (left) and supported homogeneous catalysis (right). R = reagents, P = Products.

cyclisation of enyne **8** with catalyst **7** gave quantitative conversion in the first run in acetone (Table 5, entry 2). Nevertheless, poor recyclability was achieved by this methodology. This was suspected to be related to the appearance of the second peak in the ^{31}P NMR spectra of complex **6** in this solvent after incorporation onto the MWNTs (see Figure S12 in the Supporting Information). Simultaneously, a colour change that increases over time was observed. However, XPS analysis of the used catalysts revealed the presence of gold still to be in the oxidation state I and all heteroatoms in the desired ratios. Thus, the deactivation can be attributed to internal complex rearrangement.

In accordance with Scheme 7, recyclability by the boomerang effect was also evaluated and showed that the catalyst can be recycled in dichloromethane (Schemes 5 and 6). However, a loss of activity was observed along the runs. A partial loss of the pyrene-tagged gold complex from the CNTs at the end of each run was postulated. To gain more information, each solution was analysed by ICP during successive runs of the transformation of enyne **14** into the cyclised molecule **21**. The results are given in Table 6. After

Table 6. f-MWNTs **7** analysed by ICP after each run.[a]

Run	Au leaching [ppm][b]	Gold lost [%][c]
1	5.50	16.4
2	1.23	3.7
3	0.73	2.2
4	0.93	2.8
5	1.22	3.6
Total 1–5	9.61	28.7

[a] Quantity of gold in the f-MWNTs **7** before catalysis: 33.5 ppm. [b] Leaching of gold in ppm in each catalytic cycle. [c] Percentage of gold lost in each catalytic cycle (Au leaching (ppm) divided by the initial quantity, 33.5 ppm).

the first run, substantial leaching was observed (i.e., 16%). This might be due to the presence of immobilised complexes in multiple layers with stacked pyrene units. During the first run, the molecules not in direct contact with CNT might be lost more easily and re-immobilised with more difficulty. The leaching is thereafter quite constant and fluctuates between 2 and 4%. This slow descent might explain some of the loss of catalytic activity over successive runs, although the leaching seems still rather too low to fully explain the high loss of activity observed after the second run. XPS analyses were also carried out after each catalytic run to check the quantity of the different elements and the oxidation state of the gold (Figure 2). The measurements showed that the oxidation state of gold always remained the same, namely Au^{I}. Thus, the deactivation is not a result of the oxidation or reduction to Au^{III} or Au^{0}, respectively. Secondly, the leaching was also confirmed by XPS measurements: the atomic ratio Au/C decreased after each catalytic test (see Table S4 in the Supporting Information).

To validate the crucial importance of temperature in these experiments, the cyclisation and recycling of enyne **14** under the same conditions as described previously (in accordance with Scheme 5: 2 mol% catalyst **7**, 30 min, RT) was tested without cooling to −40°C before separation of the CNTs. The second catalytic run did not give any cyclisation product, which supports the dependency of π–π stacking on temperature. ICP analysis was realised after the first catalytic run and showed gold leaching of 36%. This is much greater than after the first run with workup at −40°C (16%). It is also even more than the sum of all the leaching during five runs (sum of gold lost is 29%, Table 6). Therefore the fall in activity is understandable but its complete cancellation remains unexplained.

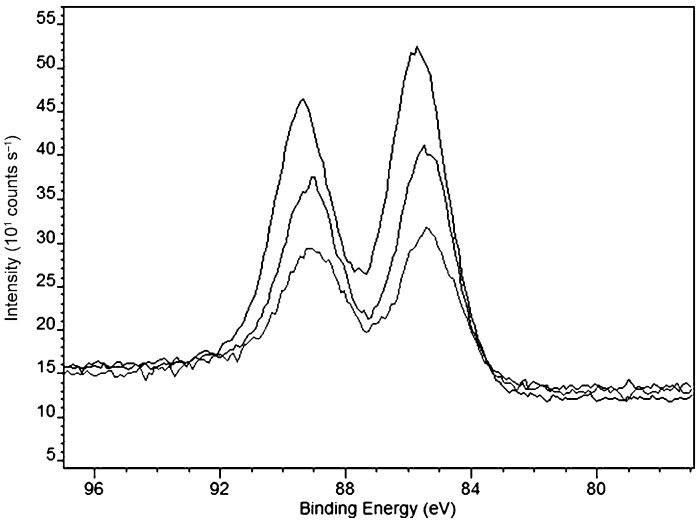

Figure 2. XPS of Au^{I} (in **7**) before catalysis (top), after two runs (middle) and after four runs (bottom).

The initial goal of this work was reached to some extent as conditions have been found for obtaining a supported homogeneous "boomerang" catalyst that is effective over successive runs. As a result of π–π interactions, the recovery of MWNTs is easily achieved by a simple change in solvent and reload of these "pristine MWNTs" with fresh pyrene-tagged gold catalyst.

Conclusion

A pyrene-tagged gold complex has been designed for immobilisation onto MWNTs through π–π interactions to give a supported homogeneous "boomerang" catalyst. This catalyst remained intact on the CNT surface after immobilisation and remarkably its activity and selectivity in cyclisation was not affected in comparison with its homogeneous counterpart. This immobilisation through pyrene allowed a boomerang effect to take place during catalysis and this effect was found to be strongly dependent on the temperature. We have shown that recycling is possible at low temperatures. To the best of our knowledge, this is the first example of a supported gold catalyst on carbon nanotubes, either by covalent or non-covalent functionalisation, and the approach could open the door to further applications.

Experimental Section

General methods: Unless otherwise stated, all the manipulations were carried out under an atmosphere of argon by using standard Schlenk techniques and with anhydrous solvents. Hexane, diethyl ether and tetrahydrofuran were distilled from sodium benzophenone under argon. Dichloromethane and acetonitrile were distilled from CaH_2. Anhydrous acetone was used as received (Fisher chemical). MWNTs were obtained from Nanocyl (Thin MWCNT, 95+% C purity). NMR spectra were recorded on Bruker spectrometers (more details can be found in the Supporting Information), HRMS were recorded on a Q-Extractive orbitrap spectrometer from ThermoFisher and XPS analyses were carried out with a SSI-X-probe (SSX 100/206) photoelectron spectrometer from Surface Science Instruments (more details can be found in the Supporting Information). ICP analyses were realised by MEDAC Ltd. (U.K.). The following compounds were obtained according to literature procedures: **8**,[66] **12**,[34] **13**,[66] **14**,[67] **15**,[34]**16**[68] and **17**.[68]

Synthesis of the bifunctional ligand 4: The first two steps, that is, compounds **2** and **3**, have been described previously.[64] 1-Pyrenebutyric acid (1.54 g, 5.35 mmol), dimethylaminopyridine (DMAP; 160 mg, 1.34 mmol) and *N*,*N*′-dicyclohexylcarbodiimide (DCC; 1.01 g, 4.91 mmol) were added to a solution of 4-diphenylphosphanylbenzylamine (**3**; 1,3 g, 4.46 mmol) in CH_2Cl_2 (40 mL). The resulting mixture was stirred at room temperature overnight. After extractive workup (1 M HCl, H_2O, 1 M NaOH, H_2O), the resulting organic phases were dried with $MgSO_4$ and thereafter purified by chromatography (95:5 CH_2Cl_2/AcOEt) to obtain **4** (2.18 g, 87%) as a pale-yellow solid. ^{1}H NMR (300 MHz, $CDCl_3$): δ = 8.28 (d, J = 9.3 Hz, 1H), 8.20–7.94 (m, 7H), 7.83 (d, J = 7.8 Hz, 1H), 7.38–7.18 (m, 14H), 5.64 (s, 1H), 4.43 (d, J = 5.7 Hz, 2H), 3.40 (t, J = 7.1 Hz, 2H), 2.36–2.17 ppm (m, 4H); ^{13}C NMR (75 MHz, $CDCl_3$): δ = 172.60, 138.91, 136.69, 135.62, 134.16, 133.90, 133.73, 133.48, 131.29, 130.77, 129.83, 128.80, 128.53, 128.44, 127.85, 127.75, 127.38, 127.33, 127.26, 126.65, 125.79, 124.86, 124.72, 123.25, 43.19, 35.69, 32.57, 27.30 ppm; ^{31}P NMR (121 MHz, $CDCl_3$): δ = −5.32 ppm; HRMS (ESI): m/z calcd for $C_{39}H_{33}O_1N_1P_1$: 562.22943 $[M+1]^+$; found: 562.22876.

Synthesis of the gold complex 6: The bifunctional ligand **4** (112 mg, 0.2 mmol) was added to a solution of $ClAuSMe_2$ (59 mg, 0.2 mmol) in CH_2Cl_2 (10 mL). The resulting mixture was stirred at room temperature for 20 min, the solvent was removed under reduced pressure and the residue vacuum-dried to obtain the gold complex **5** as a pale-yellow solid. Complex **5** was dissolved in CH_2Cl_2 (10 mL) and $AgNTf_2$ (78 mg, 0.2 mmol) was added. The mixture was stirred at room temperature for 20 min, then filtered through a millipore membrane in a disposable plastic syringe and the solution concentrated by removing most of the solvent on a Schlenk line. Hexane was added (20 mL) to induce the precipitation of **6** (176 mg, 85%) as a pale-yellow solid: ^{1}H NMR (300 MHz, $CDCl_3$): δ = 8.32–7.75 (m, 9H), 7.61–7.36 (m, 14H), 5.81 (s, 1H), 4.46 (d, J = 5.8 Hz, 2H), 3.40 (t, J = 7.2 Hz, 2H), 2.39–2.16 ppm (m, 4H); ^{13}C NMR (126 MHz, $CDCl_3$): δ = 175.73, 142.70, 135.27, 134.33, 134.22, 133.99, 133.88, 132.80, 131.35, 130.78, 129.99, 129.72, 129.62, 128.83, 128.73, 128.64, 127.50, 127.40, 127.00, 126.86, 126.47, 126.02, 125.59, 125.09, 125.00, 124.88, 123.15, 121.00, 118.44, 43.36, 35.70, 32.63, 27.89 ppm; ^{31}P NMR (121 MHz, $CDCl_3$): δ = 30.05 ppm; ^{19}F NMR (282 MHz, $CDCl_3$): δ = −75.44; HRMS (ESI): m/z calcd for $C_{39}H_{32}O_1N_1{}^{197}Au_1P_1{}^+$: 758.18815; found 758.18809; MS (ESI) m/z calcd for $C_2O_4N_1F_6{}^{32}S_2{}^-$:279.91674; found 279.91830.

General procedure for the immobilisation of the gold complex 6 onto MWNTs to obtain 7: Thin MWCNTs (95+% C purity; 100 mg, 8.33 mmol) were submitted to ultrasound for 1 h in the selected solvent (acetone, dichloromethane or acetonitrile; 30 mL). The pyrene-tagged gold(I) complex **6** was then added (100 mg, 0.1 mmol) and the resulting mixture was stirred at room temperature for various times (from 20 min to 1 day). The resulting powder was submitted to centrifugation (6500 rpm, 5 min) and washed twice with the selected solvent (6500 rpm, 5 min) to separate the non-immobilised gold complex **6** from the supported homogeneous catalyst system **7**. The resulting supported homogeneous catalyst was vacuum-dried.

General procedure for cyclisation of enynes 8 and 12–16 catalysed by the Au^I complex 6: The enyne (9.63×10^{-2} mmol) in CH_2Cl_2 (3 mL) was added to gold catalyst **6** (2 mg, 1.925×10^{-3} mmol, 2 mol%) in CH_2Cl_2 (2 mL) and the mixture was stirred at room temperature for the duration indicated in Scheme 4. The resulting mixture was filtered through SiO_2 and the solvent evaporated to give the corresponding product (**9**–**11**, **18**–**24**; see the Supporting Information). These compounds have been reported in the literature previously: **9**,[69] **10**,[66] **11**,[70] **18**,[34] **19**,[34] **20**,[34] **21**,[34] **22**,[34] **23**,[71] **24**.[71]

General procedure for the cyclisation of enynes 8 and 12–17 catalysed by the Au^I complex 6: *f*-MWNTs **7** (3.55×10^{-3} mmol, 2 mol% of supported gold complex based on ICP values, typically 20 mg) were submitted to ultrasound in CH_2Cl_2 (4 mL) for 10 min. The enyne (0.178 mmol) in CH_2Cl_2 (3 mL) was then added and the mixture stirred for 30 min (**8**, **12**–**16**) or 7 h (**17**). Agitation was then stopped and the solution was cooled to −40 °C (bath CH_3CN/N_2) for 30 min. The reaction products were separated from system **7** by centrifugation (6500 rpm, 5 min). The products were filtered through Celite and analysed by ^{1}H NMR spectroscopy.

General procedure for the recycling of catalyst 7—cyclisation of enyne 8 and 14: The procedure was carried out in accordance with Scheme 5. *f*-MWNTs **7** (3.55×10^{-3} mmol, 2 mol% of supported gold complex based on ICP values) were submitted to ultrasound in CH_2Cl_2 (4 mL) for 10 min. Enyne **8** (42 mg, 0.178 mmol) or enyne **14** (49 mg, 0.178 mmol) in CH_2Cl_2 (3 mL) was added and the mixture was stirred for 30 min. Agitation was then stopped and the solution cooled to −40 °C (bath CH_3CN/N_2) for 30 min. The mixture was submitted to centrifugation (6500 rpm, 5 min) and washed with cold CH_2Cl_2 (−40 °C, 5 mL, 6500 rpm, 5 min) to separate the reaction products from the catalyst **7**. The products were filtered through Celite (except when leaching was analysed) and analysed by ^{1}H NMR spectroscopy. The *f*-MWNTs were vacuum-dried and used in the subsequent catalytic cycles following the protocol described above.

Acknowledgements

We acknowledge the FRS-FNRS, FRIA, Fédération Wallonie-Bruxelles, Loterie Nationale, the Belgian State (IAP Project No. P6/17) and the Université catholique de Louvain for funding. We are also grateful to Nanocyl for supplying MWNTs, and to T. Haynes and J.-F. Statsijns for technical support.

[1] D. E. De Vos, M. Dams, B. F. Sels, P. A. Jacobs, *Chem. Rev.* **2002**, *102*, 3615–3640.
[2] C. E. Song, S. Lee, *Chem. Rev.* **2002**, *102*, 3495–3524.
[3] N. E. Leadbeater, M. Marco, *Chem. Rev.* **2002**, *102*, 3217–3274.
[4] A. Corma, H. Garcia, *Top Catal.* **2008**, *48*, 8–31.
[5] A. Choplin, F. Quignard, *Coord. Chem. Rev.* **1998**, *178–180*, 1679–1702.
[6] M. H. Valkenberg, W. F. Hölderich, *Catal. Rev. Sci. Eng.* **2002**, *44*, 321–374.
[7] A. Schaetz, M. Zeltner, W. J. Stark, *ACS Catal.* **2012**, *2*, 1267–1284.
[8] A. Hirsch, *Angew. Chem.* **2002**, *114*, 1933–1939; *Angew. Chem. Int. Ed.* **2002**, *41*, 1853–1859.
[9] P. Singh, S. Campidelli, S. Giordani, D. Bonifazi, A. Bianco, M. Prato, *Chem. Soc. Rev.* **2009**, *38*, 2214–2230.
[10] D. Tasis, N. Tagmataechis, A. Bianco, M. Prato, *Chem. Rev.* **2006**, *106*, 1105–1136.
[11] K. Balasubramanian, M. Burghard, *Small* **2005**, *1*, 180–192.
[12] Y. L. Zhao, J. F. Stoddart, *Acc. Chem. Res.* **2009**, *42*, 1161–1171.
[13] H. Huang, Q. Yuang, J. S. Sha, R. D. K. Misra, *Adv. Drug Delivery Rev.* **2011**, *63*, 1332–1339.
[14] C. Schulz-Drost, V. Sgobba, C. Gerhards, S. Leubner, R. M. Krieck Calderon, A. Ruland, D. M. Guldi, *Angew. Chem.* **2010**, *122*, 6569–6574; *Angew. Chem. Int. Ed.* **2010**, *49*, 6425–6429.
[15] C. Vijayakumar, B. Balan, M.-J. Kim, M. Takeuchi, *J. Phys. Chem. C* **2011**, *115*, 4533–4539.
[16] C. Janiak, *J. Chem. Soc. Dalton Trans.* **2000**, 3885–3896.

[17] D. A. Britzab, A. N. Khlobystov, *Chem. Soc. Rev.* **2006**, *35*, 637–659.
[18] Y. Ito, M. Sawamura, T. Hayashi, *J. Am. Chem. Soc.* **1986**, *108*, 6405–6406.
[19] Y. Ito, M. Sayamura, T. Hayashi, *Tetrahedron Lett.* **1988**, *29*, 239–240.
[20] S. D. Pastor, A. Togni, *J. Am. Chem. Soc.* **1989**, *111*, 2333–2334.
[21] A. Togni, S. D. Pastor, *J. Org. Chem.* **1990**, *55*, 1649–1664.
[22] A. S. K. Hashmi, L. Schwarz, J.-H. Choi, T. M. Frost, *Angew. Chem.* **2000**, *112*, 2382–2385; *Angew. Chem. Int. Ed.* **2000**, *39*, 2285–2288.
[23] A. S. K. Hashmi, T. M. Frost, J. W. Bats, *J. Am. Chem. Soc.* **2000**, *122*, 11553–11554.
[24] A. S. K. Hashmi, *Chem. Rev.* **2007**, *107*, 3180–3211.
[25] Z. Li, C. Brouwer, C. He, *Chem. Rev.* **2008**, *108*, 3239–3265.
[26] N. Krause, C. Winter, *Chem. Rev.* **2011**, *111*, 1994–2009.
[27] A. Corma, A. Leyva-Pérez, M. J. Sabater, *Chem. Rev.* **2011**, *111*, 1657–1712.
[28] E. Jiménez-Núñez, A. M. Echavarren, *Chem. Rev.* **2008**, *108*, 3326–3350.
[29] A. Arcadi, *Chem. Rev.* **2008**, *108*, 3266–3325.
[30] C. Aubert, L. Fensterbank, P. Garcia, M. Malacria, A. Simonneau, *Chem. Rev.* **2011**, *111*, 1954–1993.
[31] L. Leseurre, C.-M. Chao, T. Seki, E. Genin, P. Y. Toullec, J.-P. Genêt, V. Michelet, *Tetrahedron* **2009**, *65*, 1911–1918.
[32] M. Raducan, C. Rodriguez-Escrich, X. C. Cambeiro, E. C. Escudo-Adan, M. A. Pericàs, A. M. Ecchavarren, *Chem. Commun.* **2011**, *47*, 4893–4895.
[33] C. Nieto-Oberhuber, S. Lopez, M. Paz Muñoz, E. Jiménez-Nuñez, E. Buñuel, D. J. Cardenas, A. M. Echavarren, *Chem. Eur. J.* **2006**, *12*, 1694–1702.
[34] C. Nieto-Oberhuber, M. Paz Muñoz, S. Lopez, E. Jiménez-Nuñez, C. Nevado, E. Herrero-Gomez, M. Raducan, A. M. Echavarren, *Chem. Eur. J.* **2006**, *12*, 1677–1693.
[35] C. Nieto-Oberhuber, M. Paz Muñoz, E. Buñuel, C. Nevado, D. J. Cardenas, A. M. Echavarren, *Angew. Chem.* **2004**, *116*, 2456–2460; *Angew. Chem. Int. Ed.* **2004**, *43*, 2402–2406.
[36] C. Nieto-Oberhuber, S. Lopez, A. M. Echavarren, *J. Am. Chem. Soc.* **2005**, *127*, 6178–6179.
[37] N. Mézailles, L. Ricard, F. Gagosz, *Org. Lett.* **2005**, *7*, 4133–4136.
[38] E. Soriano, J. Marco-Contelles, *Acc. Chem. Res.* **2009**, *42*, 1026–1036.
[39] C. Li, Y. Zeng, H. Zhang, J. Feng, Y. Zhang, J. Wang, *Angew. Chem.* **2010**, *122*, 6557–6561; *Angew. Chem. Int. Ed.* **2010**, *49*, 6413–6417.
[40] S. K. Hashmi, C. Hubbert, *Angew. Chem.* **2010**, *122*, 1026–1028; *Angew. Chem. Int. Ed.* **2010**, *49*, 1010–1012.
[41] V. Lo'pez-Carrillo, N. Huguet, A. Mosquera, A. M. Echavarren, *Chem. Eur. J.* **2011**, *17*, 10972–10978.
[42] H. Duan, S. Sengupta, J. L. Petersen, N. G. Akhmedov, X. Shi, *J. Am. Chem. Soc.* **2009**, *131*, 12100–12102.
[43] L. Leseurre, P. Y. Toullec, J.-P. Genêt, V. Michelet, *Org. Lett.* **2007**, *9*, 4049–4052.
[44] N. Nishina, Y. Yamamoto, *Tetrahedron Lett.* **2008**, *49*, 4908–4911.
[45] A. Leyva, A. Corma, *J. Org. Chem.* **2009**, *74*, 2067–2074.
[46] a) A. S. K. Hashmi, W. Yang, F. Rominger, *Angew. Chem.* **2011**, *123*, 5882–5885; *Angew. Chem. Int. Ed.* **2011**, *50*, 5762–5765; b) A. S. K. Hashmi, W. Yang, F. Rominger, *Chem. Eur. J.* **2012**, *18*, 6576–6580.
[47] A. S. K. Hashmi, *Pure Appl. Chem.* **2010**, *82*, 1517–1528.
[48] P. Nun, J. D. Egbert, M.-J. Oliva-Madrid, S. P. Nolan, *Chem. Eur. J.* **2012**, *18*, 1064–1067.
[49] R. Giordano, P. Serp, P. Kalck, Y. Khin, J. Schreiber, C. Marhic, J.-L. Duvail, *Eur. J. Inorg. Chem.* **2003**, 610–617.
[50] S. Banerjee, S. S. Wong, *J. Am. Chem. Soc.* **2002**, *124*, 8940–8948.
[51] Y. Zhang, H.-B. Zhang, G.-D. Lin, P. Chen, Y.-Z. Yuan, K. R. Tsai, *Appl. Catal. A* **1999**, *187*, 213–224.
[52] C. Baleizão, B. Gigante, H. Garcia, A. Corma, *J. Catal.* **2004**, *221*, 77–84.
[53] C. Baleizão, B. Gigante, H. Garcia, A. Corma, *Tetrahedron* **2004**, *60*, 10461–10468.
[54] M. Moghadam, S. Tangestaninejad, V. Mirkhani, I. Mohammadpoor-Baltork, N. S. Mirbagheri, *J. Organomet. Chem.* **2010**, *695*, 2014–2021.
[55] M. Moghadam, S. Tangestaninejad, V. Mirkhani, I. Mohammadpoor-Baltork, N. S. Mirbagheri, *J. Mol. Catal. A* **2010**, *329*, 44–49.
[56] M. Nooraeipour, M. Moghadam, S. Tangestaninejad, V. Mirkhani, I. Mohammadpoor-Baltork, N. Iravani, *J. Coord. Chem.* **2012**, *65*, 226–238.
[57] M. Zakeri, M. Moghadam, I. Mohammadpoor-Baltork, S. Tangestaninejad, V. Mirkhani, A. R. Khosropour, *J. Coord. Chem.* **2012**, *65*, 1144–1157.
[58] M. Moghadam, I. Mohammadpoor-Baltork, S. Tangestaninejad, V. Mirkhani, H. Kargar, N. Zeini-Isfahani, *Polyhedron* **2009**, *28*, 3816–3822.
[59] G. Liu, B. Wu, J. Zhang, X. Wang, M. Shao, J. Wang, *Inorg. Chem.* **2009**, *48*, 2383–2390.
[60] F. Li, B. Zhang, X. Li, Y. Jiang, L. Chen, Y. Li, L. Sun, *Angew. Chem.* **2011**, *123*, 12484–12487; *Angew. Chem. Int. Ed.* **2011**, *50*, 12276–12279.
[61] L. Xing, J.-H. Xie, Y.-S. Chen, L.-X. Wang, Q.-L. Zhou, *Adv. Synth. Catal.* **2008**, *350*, 1013–1016.
[62] P. D. Tran, A. Le Goff, J. Heidkamp, B. Jousselme, N. Guillet, S. Palacin, H. Dau, M. Fontecave, V. Artero, *Angew. Chem.* **2011**, *123*, 1407–1410; *Angew. Chem. Int. Ed.* **2011**, *50*, 1371–1374.
[63] A. Schätz, O. Reiser, W. J. Stark, *Chem. Eur. J.* **2010**, *16*, 8950–8967.
[64] M. Nishimura, M. Ueda, N. Miyaura, *Tetrahedron* **2002**, *58*, 5779–5787.
[65] S. Kyatskaya, J. R. G. Mascaros, L. Bogani, F. Hennrich, M. Kappes, W. Wernsdorfer, M. Ruben, *J. Am. Chem. Soc.* **2009**, *131*, 15143–15151.
[66] J. W. Faller, P. P. Fontaine, *J. Organomet. Chem.* **2006**, *691*, 1912–1918.
[67] F. Monnier, C. Vovard-Le Bray, D. Castillo, V. Aubert, S. Dérien, P. H. Dixneuf, L. Toupet, A. Ienco, C. Mealli, *J. Am. Chem. Soc.* **2007**, *129*, 6037–6049.
[68] H. Yamamoto, M. Nishiyama, H. Imagawa, M. Nishizawa, *Tetrahedron Lett.* **2006**, *47*, 8369–8373.
[69] S. Gaillard, J. Bosson, R. S. Ramon, P. Nun, A. M. Z. Slawin, S. P. Nolan, *Chem. Eur. J.* **2010**, *16*, 13729–13740.
[70] M. Nishizawa, V. K. Yadav, M. Skwarczynski, H. Takao, H. Imagawa, T. Sugihara, *Org. Lett.* **2003**, *5*, 1609–1612.
[71] A. K. Buzas, F. M. Istrate, F. Gagosz, *Tetrahedron* **2009**, *65*, 1889–1901.

Received: March 15, 2013
Revised: May 21, 2013
Published online: ■■ ▮▮, 0000

